Validation of a Novel CHX-A″ Derivative Suitable for Peptide Conjugation: Small Animal PET/CT Imaging Using Yttrium-86-CHX-A″-Octreotide

Thomas Clifford,[†,§,||] C. Andrew Boswell,[†,||] Gráinne B. Biddlecombe,[‡] Jason S. Lewis,[‡] and Martin W. Brechbiel*[,†]

Radioimmune & Inorganic Chemistry Section, Radiation Oncology Branch, National Cancer Institute, Building 10 Center Drive, Bethesda, Maryland 20892-1088, and Mallinckrodt Institute of Radiology, Washington University School of Medicine, St. Louis, Missouri 63110

Received March 20, 2006

A versatile bifunctional chelating reagent based on a preorganized cyclohexyl derivative of DTPA (CHX-A″) has been developed for the convenient *N*-terminal labeling of peptides with metal ion radionuclides of Bi(III), In(III), Lu(III), or Y(III). This was achieved via the synthesis of a mono-*N*-hydroxysuccinimidyl penta-*tert*-butyl ester derivative of CHX-A″ (*trans*-cyclohexyldiethylenetriaminepenta-acetic acid) featuring a glutaric acid spacer. Commercially obtained octreotide was modified at its *N*-terminus by this reagent in the solution phase, and its subsequent radiolabeling with ^{111}In ($T_{1/2}$ = 2.8 d) and ^{86}Y ($T_{1/2}$ = 14.7 h) demonstrated. Small animal PET/CT imaging results of ^{86}Y-CHX-A″-octreotide in a somatostatin receptor-positive tumor-bearing rat model are presented for the validation of the novel agent.

Introduction

The development of improved bifunctional chelating agents for molecular imaging and targeted radiotherapy of cancer continues to progress the field of nuclear medicine. Research by Brechbiel and co-workers led to the establishment of a preorganized DTPA[a] analogue, CHX-A″ (*trans*-cyclohexyldiethylenetriaminepenta-acetic acid) (Figure 1), as the premier chelator for targeted α-particle therapy using the bismuth radionuclide, ^{213}Bi, which has shown impressive results in cancer therapy studies.[1] Furthermore, CHX-A″ forms stable and biocompatible metal complexes with the γ and Auger emitter, ^{111}In ($T_{1/2}$ = 2.8 d),[2,3] a high-energy β^--emitter, ^{90}Y ($T_{1/2}$ = 64.06 h),[2−4] the β^+-emitter, ^{86}Y ($T_{1/2}$ = 14.7 h),[3,5] and a lower-energy β^--emitter, ^{177}Lu ($T_{1/2}$ = 6.65 d),[5] making it a highly versatile chelator for radiopharmaceutical applications. Due in part to its overall acyclic structure, CHX-A″ is capable of achieving rapid complex formation with a variety of radiometals at room temperature, offering a distinct advantage over the macrocyclic chelator, DOTA (1,4,7,10-tetraazacyclododecane-1,4,7,10-tetraacetic acid).[6] Furthermore, Bi(III) complex formation kinetics with DOTA are slow and somewhat impractical for use with ^{213}Bi ($T_{1/2}$ = 45.6 min).[7,8] The characterization of the Bi(III) complex of a preorganized cyclohexyl analogue of DTPA (H_5CyDTPA) was described in 1996.[9]

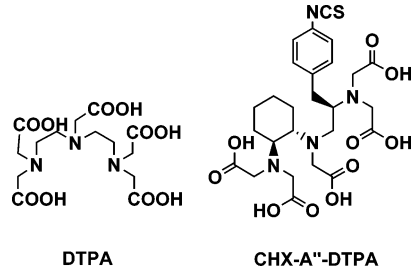

Figure 1. Structures of the parent compound (DTPA) (left) and the previously reported isothiocyanate derivative of CHX-A″ (CHX-A″-DTPA) (right).

An evaluation of antibodies labeled with ^{88}Y via conjugation to the four stereoisomers of 2-(*p*-nitrobenzyl)-*trans*-CyDTPA confirmed that the CHX-A isomers are superior to the CHX-B isomers with the CHX-A″ diastereomer clearing from the circulation slightly faster than CHX-A′, while also showing the lowest uptake by bone of any of the four diastereomers.[10,11] Thereafter, the versatility of the CHX-A″ chelate has been widely demonstrated through various applications including the stable complexation of the high-linear energy transfer (high-LET) α-emitter, ^{213}Bi,[12,13] and a variety of other radiometals (vide supra). These applications, however, feature CHX-A″ coupled exclusively to antibodies, illustrating the need for a CHX-A″-derivative that is amenable to coupling with peptides.

The targeting of somatostatin receptors (SSR) has been a goal in cancer treatment and diagnosis since the 1980s.[14−17] Somatostatin is a 14-amino acid peptide with an inhibitory role in the normal regulation of the central nervous system, the hypothalamus, the pituitary gland, the gastrointestinal tract, and the exocrine and endocrine pancreas.[18,19] In addition, SSRs are overexpressed by a number of neuroendocrine and breast tumor cells[20] and have more recently been linked to cellular proliferation and angiogenesis.[21] Octreotide is an eight-amino acid analogue of somatostatin that is highly resistant to enzymatic degradation and useful in the management of cancer.[14−17] We chose to target and image SSR expression using the β^+-emitter, ^{86}Y ($T_{1/2}$ = 14.7 h), whose intermediate half-life is well suited to octreotide-based imaging as the radioactive half-life of the isotope is reasonably matched to the biological half-life of the radiolabeled peptide conjugate.

* To whom correspondence should be addressed. Tel: 301-496-0591. Fax: (301) 402-1923. E-mail: martinwb@mail.nih.gov.
† National Cancer Institute.
‡ Washington University School of Medicine.
§ Current address: Morphix Technologies, 2557 Production Road, Virginia Beach, VA 23454.
|| These authors contributed equally to the execution of these studies.

[a] Abbreviations: DTPA, diethylenetriaminepentaacetic acid; CHX-A″, *trans*-cyclohexyldiethylenetriaminepenta-acetic acid; DOTA, 1,4,7,10-tetraazacyclododecane-1,4,7,10-tetraacetic acid; SSR, somatostatin receptor; PET, positron emission tomography; CT, computed tomography; 1B4M, 2-(4-aminobenzyl)-6-methyl-diethylenetriaminepentaacetic acid; SPPS, solid-phase peptide synthesis; OC, octreotide; Cbz, carbamazepine; Fmoc, 9-fluorenylmethyloxycarbonyl; Boc, *N-tert*-butyloxycarbonyl; EDTA, ethylenediaminetetraacetic acid; HBTU, 2-(1*H*-benzotriazol-1-yl)-1,1,3,3,-tetramethyluronium hexafluorophosphate; DMF, dimethylformamide; KOH, potassium hydroxide; TFA, trifluoroacetic acid; TLC, thin-layer chromatography; HPLC, high-pressure liquid chromatography; TMS, tetramethylsilane; TSP, sodium 3-trimethylsilyl-2,2′,3,3′-tetradeuteriopropionate; ESI, electrospray ionization; TOF, time-of-flight; MS, mass spectrometry; EDT, 1,2-ethanediol.

10.1021/jm060317v CCC: $33.50
Published on Web 06/20/2006

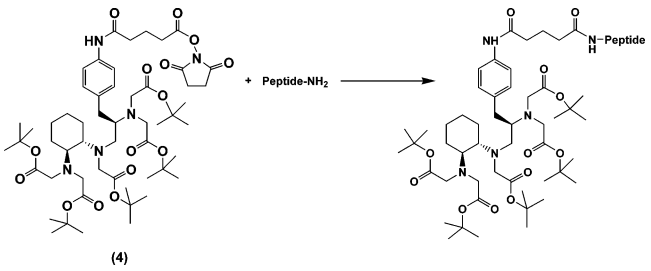

Figure 2. Schematic representation of the conjugation reaction between the novel glutaric acid succinimidyl ester derivative of CHX-A″ (**4**) and a generic *N*-terminal peptide.

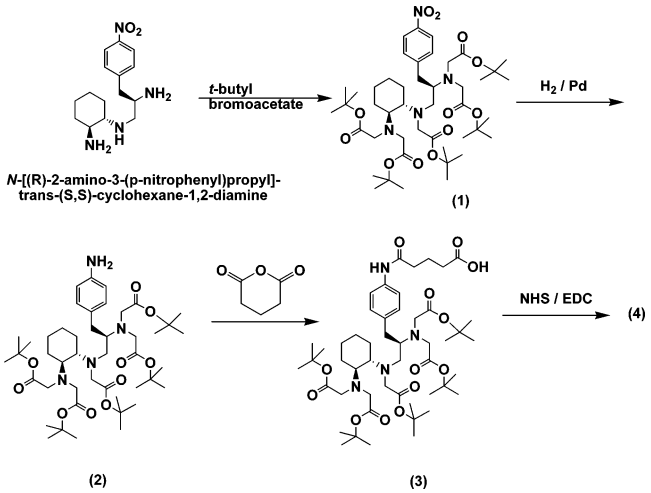

Figure 3. Schematic representation of the synthesis of **4**.

Herein, we report on the development of an improved CHX-A″ analogue widely applicable to the modification of peptides, antibodies, and other molecules via standard succinimidyl ester coupling chemistry (Figure 2). This has been accomplished by the design and synthesis of a mono-*N*-hydroxysuccinimidyl penta-*tert*-butyl ester derivative of CHX-A″ with a glutaric acid spacer moiety to lessen the steric effects and interactions of the chelator−metal complex on peptide−receptor binding affinity. The succinimidyl ester coupling chemistry is clean, efficient, and compatible with both solution and solid-phase peptide coupling techniques. This extension of the versatility of CHX-A″ bridges a gap between large macromolecules (e.g., antibodies) and smaller biomolecules (e.g., peptides) as exemplified by the targeting and imaging using the highly successful SSR-targeted peptide, octreotide.

Results

Synthesis. Characterization and structural confirmation of all key intermediates and the succinimidyl ester-containing CHX-A″ bifunctional chelating agent (Figure 3) were performed by ^{1}H NMR, ^{13}C NMR, and electrospray mass spectrometry (Supporting Information). Two-dimensional COSY (correlation spectroscopy) NMR spectra were collected for the nitro-precursor (**1**) and for the acid (**3**) (Supporting Information). Electrospray mass spectra were obtained for the protected and deprotected CHX-A″-octreotide conjugates (Supporting Information). The ^{1}H and ^{13}C NMR spectra of both the protected and deprotected CHX-A″-octreotide conjugate indicated the presence of the expected product; however, a complete peak assignment of these complicated spectra was not performed (Supporting Information). NMR spectra of simpler octreotide−chelator conjugates with complexed metal ions have been previously reported, including an NMR of Y(III)-DOTA-D-Phe^{1}-Tyr^{3}-octreotide.[22] The protected CHX-A″-octreotide conjugate was analyzed by C-18 reversed-phase HPLC and eluted in a single peak at 30 min with aqueous trifluoroacetic acid (TFA) with a CH_3CN gradient (Figure 4).

Radiolabeling and Reversed-Phase HPLC of ^{111}In-CHX-A″-octreotide. Metal ion complexation of ^{111}In was demonstrated by reversed-phase HPLC of the radiolabeled peptide under neutral pH conditions. A doublet of peaks at 23.5 and 24 min was observed for ^{111}In-CHX-A″-octreotide on a reversed-phase HPLC eluting with aqueous ammonium acetate and an increasing acetonitrile gradient (Figure 5). The time-resolution of two distinct radioactive species may be attributed to the emergence of two structural isomers of CHX-A″-octreotide upon In(III) complexation. Reversed-phase HPLC resolution of two isomeric forms of a similar In(III)-DTPA-peptide conjugate has been recently documented.[23]

Radiosynthesis and Characterization of ^{86}Y-CHX-A″-octreotide. Radiolabeling was achieved via the incubation of CHX-A″-octreotide with $^{86}YCl_3$ in 0.5 M NH_4OAc at 25 °C. Quality control of the product was performed using radio thin-layer chromatography on $MKC_{18}F$ silica gel plates (2.5 × 7.5 cm) using NH_4OAc/methanol (30:70) as the eluent. Radiochemical yields greater than 97% (0.1 mCi/μg; 6.49 × 10^{6} MBq/mmole) for ^{86}Y-CHX-A″-octreotide were obtained by this method.

Small Animal PET/CT Co-Registration Imaging. The ^{86}Y-dependent PET images were co-registered with computed tomography (CT) images to aid in anatomical interpretation of the imaging results. The uptake of ^{86}Y-CHX-A″-octreotide in SSR-bearing AR42J tumors is clearly visible in both axial

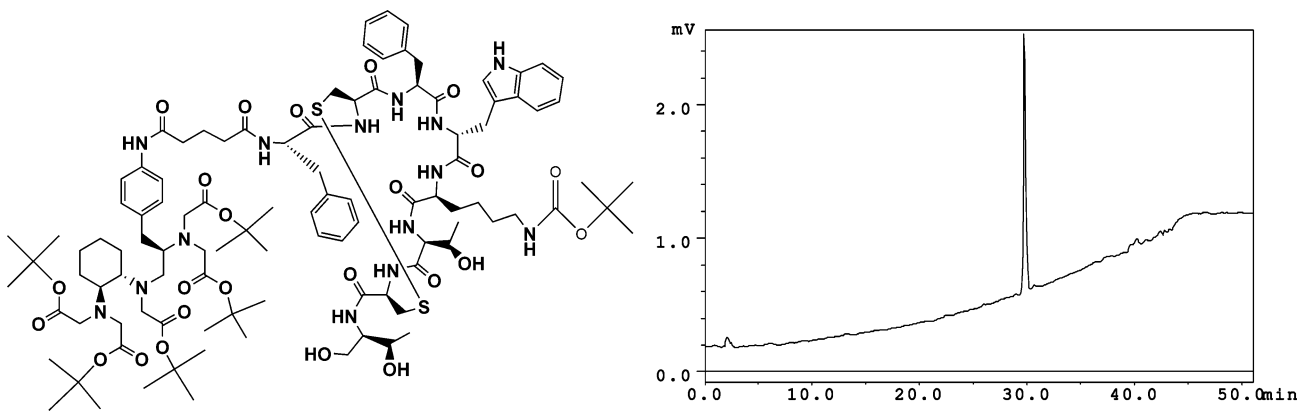

Figure 4. Structural representation (left) and UV elution profile (right) of protected CHX-A″-octreotide resulting from the reaction of **4** with octreotide.

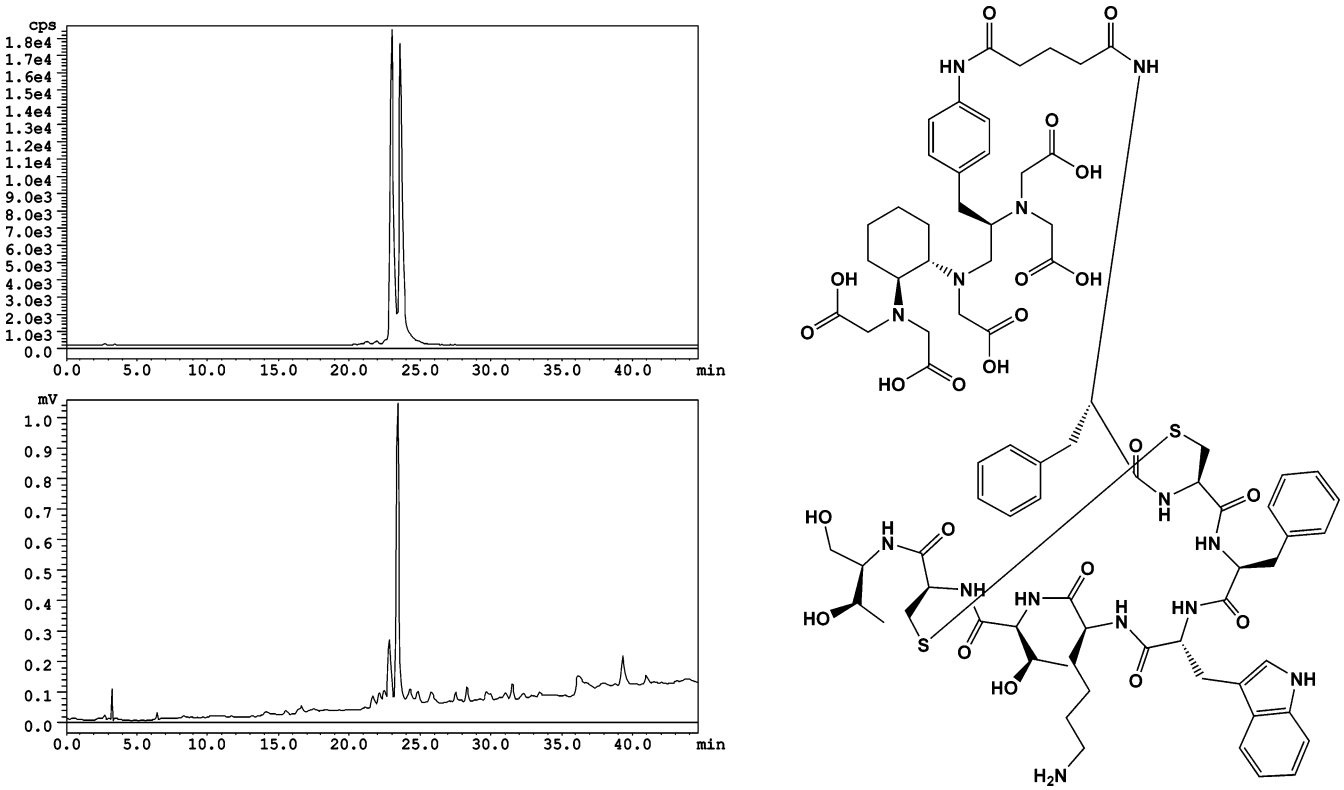

Figure 5. Radioactive (top) and UV (bottom) elution profiles of ^{111}In-CHX-A″-octreotide. A structural representation of deprotected CHX-A″-octreotide is also shown (right).

(Figure 6) and coronal (Figure 7) views at 4 h postinjection. Significant accumulation of ^{86}Y-CHX-A″-octreotide was also observed in the kidneys (Figures 6 and 7). The images of animals receiving a blocking injection of octreotide still demonstrated an uptake in clearance organs (kidneys) but not in tumors (Figures 6 and 7).

Biodistribution Studies of ^{86}Y-CHX-A″-octreotide. The uptake of ^{86}Y-CHX-A″-octreotide in SSR-positive organs at 4 h postinjection expressed as percent injected dose per gram (%ID/g) are as follows: the pituitary gland (1.70 ± 0.08), adrenal glands (0.95 ± 0.30), and pancreas (0.65 ± 0.24) (Figure 8; Supporting Information). Accumulation was also observed in the AR42J tumor (0.94 ± 0.22) and the kidneys (20.38 ± 5.62) (Figure 8; Supporting Information). At 24 h postinjection, the majority of the agent had mostly cleared the kidneys (3.90 ± 0.04), pituitary (0.22 ± 0.01), pancreas (0.12 ± 0.03), adrenals (0.06 ± 0.01), and the tumor (0.07 ± 0.01) (Figure 8; Supporting Information).

Discussion

The radiolabeling of antibodies following conjugation with isothiocyanate derivatives of 1B4M (2-(4-aminobenzyl)-6-methyl-diethylenetriaminepentaacetic acid) and CHX-A″ (Figure 1) has been thoroughly investigated in our laboratory.[1,2,10−13,15,24] This strategy, however, was not readily applicable to solid-phase peptide synthesis (SPPS) because there were concerns that the thiourea conjugate would undergo Edman degradation under TFA cleavage and deprotection conditions during conventional Fmoc SPPS. The penta-*tert*-butyl ester derivative of CHX-A″ with a glutaric acid spacer moiety was chosen as an alternate chelator precursor. After converting the terminal carboxylate to an activated ester (Figure 3), the reagent could be used in a conventional peptide synthesizer to modify a peptide at the *N*-terminus (Figure 2) prior to cleavage of the peptide from the polymer support. Alternatively, the reagent may be reacted in solution phase following cleavage from hyper-acid sensitive resins with peptides still having protection intact on reactive residues (e.g., BOC-protected lysines) but whose *N*-terminus is available for reaction. In this specific article, we chose to highlight this latter scenario using the eight-amino acid somatostatin analogue, octreotide, as a prototype.

Solid-phase labeling strategies for the construction of peptides with inherent metal ion chelators can facilitate the high-throughput screening of putative molecular imaging agents generated from peptide libraries. An amino acid analogue designed to incorporate *p*-aminobenzyl-EDTA into proteins has been previously described.[26] Similar strategies for the solid-phase introduction of Re and/or ^{99m}Tc chelators have also been explored.[27,28] A more recent report describes the convenient solid-phase synthesis of a DTPA-conjugated peptide and labeling with the γ-emitter, ^{111}In.[23] Herein, we have described a novel CHX-A″ agent that serves to extend this concept to real-time imaging with improved resolution by PET using ^{86}Y. In addition, this CHX-A″ DPTA analogue potentially creates a facile synthetic route to a variety of α- and β-emitting targeted agents for radiotherapeutic applications.

The structures of both peptide and chelate play critical roles in determining the success of radiolabeled peptides in nuclear medicine. The chemical properties of the chelate−metal complex (e.g., lipophilicity, charge, size, steric bulk, etc.) do indeed have an important impact, especially for small peptides. In addition, the requirement for rapid and kinetically stable chelation is necessary to prevent the escape of radiometal ions and subsequent accumulation into nontarget organs.[29] The promising small animal PET imaging results presented in this article suggest (1) that this peptide-CHX-A″ conjugate formed a stable ^{86}Y complex that allowed for tumor specific targeting and next-day clearance and (2) that the structure of this CHX-A″ derivative did not adversely affect the SSR targeting properties of octreotide.

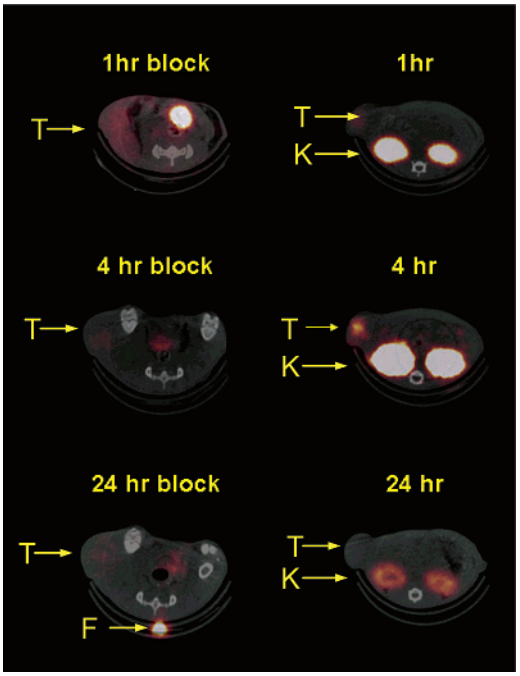

Figure 6. Axial slices of small animal PET/CT coregistration images of an AR42J-bearing rat at 1, 4, and 24 h following the intravenous injection of ^{86}Y-CHX-A″-octreotide with (left) and without (right) an octreotide block. The images shown are 1 mm slices with the animal in the supine position, and the slices shown are through the center of the tumor volume. Because tumors do not grow in exactly the same location from animal to animal, the slices may show different tissues in addition to the tumors. The PET images show that the administration of a blockade dose substantially reduces the tumor uptake of the agent by such an extent that the tumor cannot be delineated. It is also evident that the background accumulation is very low (i.e., low nontarget tissue uptake) except for activity in the kidneys, consistent with the biodistribution data. Very little activity was delineated in any other tissues in the imaging studies. The acute biodistribution data did indicate accumulation of the agent into other SSR-rich tissues, such as the adrenals, pituitary, and pancreas; however, these were not visualized by the imaging because of the pituitary not being in the field of view, the diffuse nature of the pancreas, and the inability to resolve the adrenals because of their proximity to the kidneys. (T, tumor; K, kidney; F, fiducial marker).

One of the most widely used γ-scintigraphy radioisotopes in radiopharmaceutical studies is ^{111}In, which decays by electron capture with the emission of γ photons of 173 and 247 keV (89% and 95% abundance, respectively). Targeted tumor radiotherapy may be achieved because of the subcellular-range Auger electron emissions that are a consequence of ^{111}In electron capture decay.[30−32] Octreotide has been labeled with both ^{123}I [33] and ^{111}In[34] and used to image SSR-positive tumors in humans.[35] Iodine-123-Tyr^3-octreotide has a high hepatobiliary excretion that hinders the visualization of tumors in the abdomen, whereas ^{111}In-DTPA-D-Phe^1-octreotide (^{111}In-DTPA-OC) clears primarily through the kidneys[35] and is currently used routinely as an imaging agent for neuroendocrine cancer. The infusion of lysine and arginine may be used to lower the radiation dose to the kidneys.[36]

There have also been reports of targeted radiotherapy studies in animal models using ^{90}Y-labeled octreotide conjugates[37,38] and ^{188}Re labeled to another SSR ligand, RC-160. ^{90}Y-DOTA-Tyr^3-octreotide (^{90}Y-DOTA-Y3-OC) was found to induce the complete remission of a rat pancreatic tumor in 70% of rats administered 10 mCi/kg[38] and has been in clinical trials in the U. S. and Europe with favorable results.[39] Recent studies have demonstrated the advantages of ^{86}Y-labeled over ^{111}In-labeled

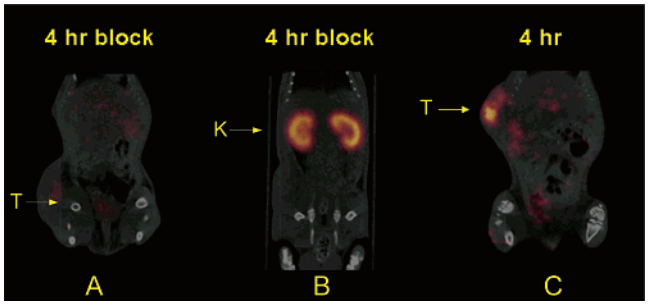

Figure 7. Coronal slices of small animal PET/CT coregistration images of an AR42J-bearing rat at 4 h following the intravenous injection of ^{86}Y-CHX-A″-octreotide with (left, center) and without (right) an octreotide block. The images shown are 1 mm slices with the animal in the supine position, and images A and C are slices through the center of the tumor volume. Image B is a slice chosen through the center of the kidneys. The PET images show that the administration of a blockade dose substantially reduces the tumor uptake of the agent by such an extent that the tumor cannot be delineated (A). It is also evident that background accumulation is very low (i.e., low nontarget tissue uptake) except for activity in the kidneys (B), consistent with the biodistribution data. The acute biodistribution data did show accumulation of the agent into other SSR-rich tissues, such as the adrenals, pituitary, and pancreas; however, these were not visualized by the imaging because of the pituitary not being in the field of view, the diffuse nature of the pancreas, and the inability to resolve the adrenals because of their proximity to the kidneys. (T, tumor; K, kidney)

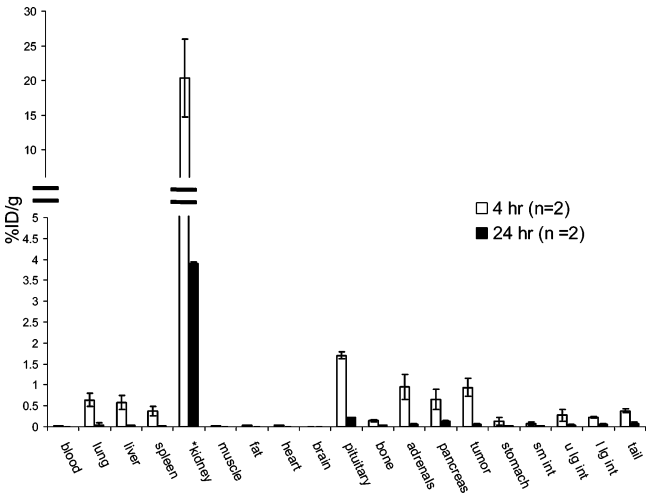

Figure 8. Biodistribution profile of AR42J-bearing rats at 4 and 24 h following the intravenous injection of ^{86}Y-CHX-A″-octreotide.

octreotides for therapy planning by comparing biodistribution and dosimetry data.[40]

The advantages of β^+-emitting somatostatin analogues include increased image resolution with positron emission tomography (PET) compared to γ-scintigraphy, improved quantification capabilities with PET, and the ability to use β^+-emitters as companion isotopes to therapeutic radionuclides such as the ^{86}Y (PET)/^{90}Y (therapy) pair.[41] Yttrium-90 has shown therapeutic efficacy as a radionuclide for both radioimmunotherapy and peptide radiotherapy. The high energy and long range of the β^- particle are probably most ideal for large tumor burdens and may not be ideal for smaller tumors.[30,42] Furthermore, because ^{90}Y emits only β^- particles (E_{max} = 2.27 MeV), tumor imaging and dosimetry calculations have usually been performed using the γ-emitter, ^{111}In. Subtle differences between the biodistributions of ^{111}In- and ^{90}Y-labeled monoclonal antibodies have been noted that may lead to discrepancies in dosimetry calculations.[43,44] In the case of targeted radiotherapeutic agents with short biological half-lives, the ^{90}Y uptake and dosimetry

could be better quantitated by PET by the prior or coadministration of the analogous ^{86}Y-labeled compound.[45] Yttrium-86 (β^+ 34% (1.248 MeV, 14%); EC 66%) has been produced by the irradiation of an enriched $^{86}SrCO_3$ target, followed by purification by a combined coprecipitation and ion-exchange purification process.[46] A Sr(II)-selective resin has also been employed for ^{86}Y purification,[47,48] and an electrochemical purification was recently reported that results in even higher chemical purity.[49] Recently, no-carrier-added, high-specific activity ^{86}Y has been produced in high yield from SrO, followed by electrochemical separation on a biomedical cyclotron.[50] A ^{86}Y-labeled cyclic peptide analogue of α-MSH, ^{86}Y-DOTA-ReCCMSH(Arg^{11}), demonstrated a much higher tumor-to-background ratio than the corresponding ^{64}Cu-labeled peptide,[51] a result attributed to the relative kinetic stability of Y(III)-DOTA[7] versus Cu(II)-DOTA.[52]

In the small animal imaging and biodistribution studies, ^{86}Y-CHX-A″-OC demonstrated high tumor concentration along with uptake in the kidney associated with the renal clearance of the agent (Figures 6−8; Supporting Information). Very little activity was delineated in any other tissues in the imaging studies. The biodistribution data indicated the accumulation of the agent into other SSR-rich tissues, such as the adrenal, pituitary, and pancreas (Figure 8; Supporting Information), although these were not visualized by the imaging because of the pituitary not being in the field of view, the diffuse nature of the pancreas, and the inability to resolve the adrenals because of their proximity to the kidneys. Tumor uptake was significantly reduced by the co-injection of a block due to the saturation of the SSR binding sites (Figure 6). This reduction in tumor uptake confirms that tumor concentration is receptor-mediated. The mass of agent administered (biodistribution = 100 ng; small animal PET = 3000 ng) was not optimal because of the final labeling specific activity of only 0.1 mCi/μg of ^{86}Y-CHX-A″-OC. In the experiments described herein, the separation of the ^{86}Y-CHX-A″-OC from unlabeled CHX-A″-OC was not attempted because of the high radiochemical purity (97%) achieved in the labeling. However, even at this level of specific activity, significant blocking of the receptor is not anticipated until higher masses of the agent are administered[53] as demonstrated by good tumor accumulation and visualization. The uptake of somatostatin peptides into tumor and other receptor-rich tissues often follows a bell-shaped relationship,[54] and at the levels given in this study, the uptake is thought to be on the fall-slide of this curve. The optimization of tumor accumulation and, as a consequence, improved delineation of the tumor in PET imaging could be improved by increasing the specific activity of the ^{86}Y-labeled peptide by the separation of the radiolabeled peptide from the nonlabeled one.

Conclusion

In summary, a novel somatostatin analogue developed in our laboratory, CHX-A″-octreotide, permits the use of the β^+-emitter ^{86}Y as an elementally matched companion isotope with the therapeutic radionuclide ^{90}Y (therapy).[41] Like the previously reported DOTA-octreotide derivatives, CHX-A″-octreotide allows for the complexation of In(III), Lu(III), or Y(III). In addition, CHX-A″-octreotide provides direct access to a selection of α-emitting radionuclides including ^{213}Bi, which has shown impressive results[1,12] in targeted α-particle therapy. The preclinical evaluation of a ^{213}Bi-labeled DOTA-octreotide derivative has already been reported;[55] however, CHX-A″ is superior to DOTA for the complexation of ^{213}Bi ($T_{1/2}$ = 45.6 min) because of more rapid complexation kinetics at ambient temperature.[7,8] Future studies involving CHX-A″-peptide conjugates labeled with α-emitting isotopes such as ^{213}Bi may lead to the development of improved targeted radiotherapeutic agents.

Experimental Methods

Materials. Mono-Boc-1,2-*trans*-(*S*,*S*)-diaminocyclohexane was prepared via bis(Cbz)-mono-Boc-1,2-*trans*-(*S*,*S*)-diaminocyclohexane as previously described[73] and was used in the synthesis of the triamine *N*-[(*R*)-2-amino-3-(*p*-nitrophenyl)propyl]-*trans*-(*S*,*S*)-cyclohexane-1,2-diamine as previously reported.[19] *Tert*-butyl bromoacetate was purchased from Fluka (Buchs, Switzerland). The HBTU coupling reagent was purchased from EMD Biosystems (San Diego, CA). DMF (Aldrich, 99%) was distilled at reduced pressure prior to use in peptide couplings. Piperidine and diisopropylethylamine were distilled from KOH. Lys(Boc) octreotide, and (Cys^2-Cys^7)*H*-D-Phe-Cys-Phe-D-Trp-Lys(Boc)-Thr-Cys-Thr-ol was purchased from Advanced ChemTech (Louisville, KY). Reagent K cleavage solution (TFA−phenol−thioanisole−EDT−H_2O, 82.5:5:5:2.5:5) was prepared immediately prior to use in the deprotection and cleavage of peptides from resin support. All other reagents were purchased from Aldrich (St. Louis, MO) and used as received.

Chemistry. Column chromatography was performed on Merck 60 Silica Gel deactivated by washing with 10% aqueous EtOH followed by air-drying to a free flowing powder over 7 days. TLC was performed on Merck Silica Gel 60 F254 glass plates visualized by UV fluorescence or development by I_2. HPLC was performed using a Beckman System Gold (Fullerton, CA) equipped with a Model 126 Solvent Delivery Module and a Model 168 UV detector (λ 254 and 280 nm) controlled by 32 Karat software.

^{1}H and ^{13}C NMR data were obtained using a Varian Gemini 300 MHz instrument, and the chemical shifts are reported in ppm on the δ scale relative to those of TMS, TSP, or the solvent. Proton chemical shifts are annotated as follows: ppm (multiplicity, integral, coupling constant (Hz)). Mass spectra were obtained on a Waters LCT Premier Time-of-Flight Mass Spectrometer using electrospray ionization (ESI/TOF/MS) operated in positive ion mode. The electrospray capillary voltage was 3 kV, and the sample cone voltage was 60 V. The desolvation temperature was 225 °C, and the desolvation gas flow rate was nitrogen at 300 L/h. Accurate masses were obtained using the lock spray mode with Leu-Enkephalin as the external reference compound.

The peptides were purified on a Waters Deltaprep 3000 preparative HPLC system using a Waters DeltaPak 15 μm C_{18} 100A 30 mm × 300 mm column 30 × 150 mm C_{18} reversed-phase connected to a Waters 750 UV/vis detector monitoring at 254 nm. The purification of *tert*-butyl-ester-protected CHX-A″-octreotide was achieved using a binary solvent gradient of 50−100% B/25 min (A = 1% aqueous TFA, B = 1% TFA in CH_3CN) at 40 mL/min. The purification of deprotected CHX-A″-octreotide was achieved using a binary solvent gradient of 10−100% B/25 min (A = 1% aqueous TFA, B = 1% TFA in CH_3CN) at 40 mL/min. Data were output to a strip chart recorder, and the relevant aliquots of the major products were collected by hand.

Analytical HPLC of *tert*-butyl-ester-protected CHX-A″-octreotide was performed using a Beckmann C_{18} reversed-phase column and a binary gradient system of 50−100% B/25 min (solvent A = 1% aqueous TFA, solvent B = 1% TFA in CH_3CN). The deprotected peptides were analyzed using a Beckmann C_{18} reversed-phase column and either of two binary solvent gradient systems of 0−100% B/40 min at 1 mL/min: (1) an acidic system where A = 1% aqueous TFA, B = 1% TFA in CH_3CN or (2) a neutral system where A = aqueous 15 mM NH_4OAc at pH 7.0, B = CH_3CN. The latter solvent gradient system was also utilized for the chromatographic analysis of peptides labeled with radiometals (vide infra).

General Procedure for Solution Phase Tagging. In brief, peptides with side chain protection intact were purchased, and the *N*-terminus appended with chelate **4** by simply mixing 1.5 equivalents of chelate **4** with the peptide in DMF. Typically ∼100 mg of peptide would be suspended in DMF (∼1 mL), and chelate **4** was added in one portion. The suspension would clear after 10−

30 min. The reaction was allowed to proceed for a total of 6−8 h, and the crude product was isolated by precipitation from diethyl ether. The Boc and *tert*-butyl ester groups were cleaved using TFA−phenol−thioanisole−EDT−H_2O following the same procedure used for resin cleaved products. The crude products were purified by reversed-phase C_{18} chromatography using aqueous TFA (1%) with an increasing CH_3CN gradient in the mobile phase. This general strategy was applied to a 100-mg sample of commercially obtained octreotide with Boc-protection on the lysine residue intact.

Radiosynthesis and Characterization of ^{111}In-CHX-A″-octreotide. A 200-μCi portion of ^{111}In (Perkin-Elmer, Wellesley, MA) in 0.05 N HCl was added to a 100-μg portion of CHX-A″-octreotide dissolved in 0.15 M NH_4OAc at pH 7. The purpose of this low specific-activity labeling was to correlate the UV and radiometric peaks of CHX-A″-octreotide and ^{111}In-CHX-A″-octreotide, respectively. The reaction mixture was incubated at 25 °C for 30 min. An aliquot of the resulting solution was analyzed by RP-HPLC using a Vydac Protein & Peptide C_{18} column equilibrated with 0.015 M NH_4OAc (pH 7). A gradient of CH_3CN that increased from 0% at 0 min to 100% at 40 min was employed, followed by an additional 10-min plateau at 100% CH_3CN. A UV detector and radiometric detector were coupled to measure absorbance at 254 nm and radioactivity, respectively.

^{86}Y Production. ^{86}Y was produced on a CS-15 biomedical cyclotron at Washington University School of Medicine using published methods.[64] Radioactivity was measured with a Capintec radioisotope calibrator and a Beckman 8000 gamma counter.

Radiosynthesis and Characterization of ^{86}Y-CHX-A″-octreotide. Radiolabeling was achieved via the incubation of CHX-A″-octreotide (20 μg) with $^{86}YCl_3$ (2.0 mCi) in a 100-μL aliquot of 0.5 M NH_4OAc (pH 5.5) at 25 °C for 1 h. Quality control of the product was performed using radio thin-layer chromatography on $MKC_{18}F$ silica gel plates (2.5 × 7.5 cm) using NH_4OAc/methanol (30:70) as the eluent.

Biodistribution Studies of ^{86}Y-CHX-A″-octreotide. All animal experiments were conducted in compliance with the Guidelines for the Care and Use of Research Animals established by Washington University's Animal Studies Committee. The biodistribution studies were conducted in male (144−163 g) Lewis rats (Charles River Laboratories, Wilmington, MA) that had been subcutaneously implanted with 2−3 mm AR42J tumor pieces into the right flank. The tumors were allowed to grow for 10 days postimplantation, at which time, the animals received 10 μCi (100 ng) of ^{86}Y-CHX-A″-octreotide in 100 μL of saline via lateral tail-vein injection. The animals were euthanized at desired time points (4 and 24 h).

Imaging Studies. Small animal PET images in AR42J-bearing rats were obtained on a microPET-Focus 220 (Concorde MicroSystems Inc., Knoxville, TN)[74] and were coregistered with CT images from a MicroCAT II System (ImTek Inc., Knoxville, TN). The animals received 300 μCi (3000 ng) of ^{86}Y-CHX-A″-octreotide in 100 μL of saline via lateral tail-vein injection. A second group of animals were pretreated with a blocking dose of 125 μg of [Tyr^1]-somatostatin (Sigma, St. Louis, MO) in 150 μL of saline immediately prior to injection with ^{86}Y-CHX-A″-octreotide.

***N*-[(*R*)-2-Amino-3-(*p*-nitrophenyl)propyl]-*trans*-(*S*,*S*)-cyclohexane-1,2-diamine-*N*,*N*,*N*′,*N*″,*N*″-penta-*tert*-butyl Acetate (1).** *N*-[(*R*)-2-Amino-3-(*p*-nitrophenyl)propyl]-*trans*-(*S*,*S*)-cyclohexane-1,2-diamine•3HCl (2.00 g, 5 mmol) stirred in acetonitrile (50 mL) with K_2CO_3 (6.21 g, 45 mmol) was treated with *tert*-butyl bromoacetate (5.17 mL, 6.83 g, 35 mmol) and stirred vigorously for 3 days. The solvent was evaporated at reduced pressure, and diethyl ether (100 mL) was added and the mixture filtered. The inorganic salts were washed with additional portions of diethyl ether (3 × 10 mL) and the filtrate evaporated at reduced pressure to produce a viscous orange oil. Purification was achieved on a silica gel column (previously treated with 10% aqueous ethanol and then rinsed with 100% ethanol followed by ethyl acetate) eluting with 30% ammonia in EtOH/EtOAc/Hexane 1:1:16 to 1:1:8 gradient (2.67 g, 62%). ^{1}H NMR (300 MHz, $CDCl_3$) δ 1.15−1.0 (br m, 4H), 1.40 (s 18H), 1.43 (s, 18H), 1.44 (s, 9H), 1.7 (br s, 4H), 2.5−2.9 (m, 4H), 2.95−3.05 (m, 1H), 3.24 (s, 2H), 3.40 (s, 2H), 3.41 (s, 2H), 3.46 (dd, J_a = 14.4 Hz, J_b = 2.7 Hz, 2H), 3.53 (s, 4H), 7.55 (d, J = 9 Hz, 2H), 8.07 (d, J = 8.7 Hz, 2H, Ph); ^{13}C NMR (75 Hz, $CDCl_3$) δ 26.114, 26.22, 26.83, 36.79, 42.16, 51.60, 52.74, 53.43, 54.12, 60.12, 62.48, 63.99, 80.39, 80.58, 80.65, 123.10, 130.77, 146.14, 151.17, 171.40, 171.76, 172.05. Anal. Calcd. for $C_{45}H_{74}N_4O_{12}$: C, 62.62; H, 8.64; N, 6.49. Found: C, 62.84; H, 8.85; N, 6.43. ES-MS: [M + H$^+$] requires, 863.53812; found, 863.5381.

***N*-[(*R*)-2-Amino-3-(*p*-aminophenyl)propyl]-*trans*-(*S*,*S*)-cyclohexane-1,2-diamine-*N*,*N*,*N*′,*N*″,*N*″ -penta-*tert*-butyl Acetate (2).** Pd on carbon (10%) was placed in an all glass hydrogenation vessel with EtOH (20 mL) charged with H_2. After the saturation of the catalyst with H_2, a solution of (**1**) (2.4 g, 2.82 mmol) in EtOH (25 mL) was injected and the pressure maintained at room pressure over 8 h by the periodic refilling with H_2. The mixture was left vigorously stirring overnight and then filtered through Celite washing with EtOH (5 × 5 mL). The filtrate was evaporated at reduced pressure to give a pale, yellow oil. The product was purified on neutral alumina eluting with hexane/EtOAc/NH_3 in EtOH in a 18:2:1 ration yielding a colorless oil after evaporation (2.29 g, 97%). ^{1}H NMR (300 MHz, $CDCl_3$) δ 1.09 (d, J = 6.9 Hz, 4H), 1.26 (d, J = 2.3 Hz, 2H), 1.43 (br s, 45H, tBu), 1.66 (br s, 2H), 2.03 (br t, J = 12 Hz, 2H), 2.5−2.7 (m, 4H), 2.75−2.9 (m, 2H), 3.05 (p, J = 6 Hz, 1H), 3.20−3.65 (m, 11H); ^{13}C NMR (75 Hz, $CDCl_3$) δ 14.26, 22.78, 25.95, 26.14, 27.35, 28.27, 28.30, 29.89, 31.72, 36.08, 52.29, 53.38, 53.71, 54.09, 62.97, 63.02, 64.34, 80.15, 80.31, 115.26, 130.34, 131.52, 144.104, 171.67, 171.98, 172.40. Anal. Calcd. for $C_{45}H_{76}N_4O_{10}$: C, 64.88; H, 9.19; N, 6.73. Found: C, 64.96; H, 9.19; N, 6.87. ES-MS: [M + H$^+$] requires, 833.56394; found, 833.5640.

***N*-[(*R*)-2-Amino-3-(*p*-aminophenyl-*N*-{5-oxopentanoic acid})-propyl]-*trans*-(*S*,*S*)-cyclohexane-1,2-diamine-*N*,*N*,*N*′,*N*″,*N*″-penta-*tert*-butyl Acetate (3).** Compound **2** (11.2 g, 12.98 mmol) and excess glutaric anhydride (2.96 g, 25.96 mmol) were mixed in benzene (60 mL) with stirring overnight. A further portion of benzene was added (60 mL), and the organic layer was washed with 0.1 M Na_2HPO_3 (1 × 30 mL) followed by washing with 0.1 M NaH_2PO_3 (2 × 30 mL). The organic fraction was dried over Na_2SO_4, filtered, and then evaporated at reduced pressure to yield a pale brown oil. The product was further purified by chromatography on a silica gel column (prepared as described above) eluting with EtOH/hexane 1:5 to 1:1 gradient yielding after evaporation at reduced pressure a glassy colorless solid (8.61 g, 71%). ^{1}H NMR (300 MHz, DMSO-d_6, TMS) δ 1.04 (σ, 4H), 1.37 (s, 45H), 1.58 (br s, 2H), 1.78 (p, J = 7.3 Hz, 2H), 1.90 (br s, 2H), 2.21 (t, J = 7.4 Hz, 2H), 2.30 (t, J = 7.4 Hz, 2H), 2.40 (dd, J_a = 12.9 Hz, J_b = 6.6 Hz, 1H), 2.58 (m, 3H), 2.73 (br d, J = 9.3 Hz, 1H), 2.8−3.0 (m, 2H), 3.12 (br d, J = 17.1 Hz, 1H), 3.28 (d, J = 9.6 Hz, 1H), 3.32 (s, 2H), 3.34 (s, 2H), 3.42 (s, 4H), 4.0 (br s, H_2O), 7.14 (d, J = 8.4, 2H) 7.45 (d, J = 8.4 Hz, 2H), 9.81 (s, 1H); ^{13}C NMR (75 Hz, DMSO-d_6, TMS) δ 20.90, 25.28, 25.47, 26.48, 27.69, 27.73, 27.87, 28.83, 31.28, 33.77, 35.31, 35.66, 52.77, 53.13, 53.34, 54.71, 62.27, 62.42, 63.01, 79.57, 79.69, 79.83, 118.49, 129.20, 135.53, 136.98, 107.55, 170.04, 171.67, 174.67. Anal. Calcd. for $C_{50}H_{82}N_4O_{13}$•(C_2H_5OH): C, 62.88; H, 8.93; N, 5.64. Found C, 62.91; H, 8.78; N, 5.59. ES-MS: [M + H$^+$] requires, 947.59563; found, 947.5957.

***N*-[(*R*)-2-Amino-3-(*p*-5-[(2,5-dioxopyrrolidin-1-yl)oxy]-5-oxo-*N*-phenylpentanamide) propyl]-*trans*-(*S*,*S*)-cyclohexane-1,2-diamine- *N*,*N*,*N*′,*N*″,*N*″-penta-*tert*-butyl Acetate. (4).** 1-[3-(dimethylamino)propyl]-3-ethylcarbodiimide hydrochloride (0.47 g, 2.45 mmol), *N*-hydroxysuccinimide (0.25 g, 2.16 mmol), and **3** (1.86 g, 1.96 mmol) were stirred in a mixture of EtOAc (90 mL) and DMF (30 mL) overnight. The reaction mixture was then diluted with ethyl acetate (30 mL) and cooled in an ice bath. The cooled mixture was washed with ice-cold 5% w/v aqueous $NaHCO_3$ (2 × 20 mL) and then with ice-cold water (2 × 20 mL). The organic fraction was dried over Na_2SO_4, filtered, and evaporated at reduced pressure to yield a glassy pale yellow solid (1.61 g, 84%). No further purification was performed on this compound. ^{1}H NMR (300 MHz, DMSO-d_6, TMS) δ1.05 (br s, 4H), 1.38 (s 36H), 1.38 (s, 9H), 1.60

(br s, 2H), 1.92 (p, $J = 9$ Hz, 2H), 2.41 (t, $J = 7.2$ Hz, 2H), 2.52−2.66 (m, 2H), 2.75 (t, $J = 7.2$ Hz, 2H), 2.82 (s, 4H), 2.85−3.04 (m, 2H), 3.1−3.5 (m, 12H), 7.176 (d, $J = 8.4$ Hz, 2H), 7.45 (d, $J = 8.4$ Hz, 2H), 9.80 (s, 1H); ^{13}C NMR (75 Hz, DMSO-d_6, TMS) δ 20.14, 25.27, 25.43, 26.60, 27.68, 27.72, 29.60, 34.59, 35.35, 52.71, 53.02, 53.36, 62.12, 62.32, 62.82, 79.44, 79.56, 79.70, 118.46, 129.212, 135.77, 136.76, 168.74, 169.80, 170.19, 170.96, 171.50. Anal. Calcd. for $C_{54}H_{85}N_5O_{15}\cdot(C_2H_5OH)$: C, 61.69; H, 8.41; N, 6.42. Found C, 61.51 H, 8.40 N, 6.63. ES-MS: [M + H$^+$] requires, 1044.61201; found, 1044.6120.

***N*-[CHX-A″ penta-*tert*-butyl ester]-(Cys2-Cys7)-D-Phe-Cys-Phe-D-Trp-Lys(Boc)-Thr-Cys-Thr-ol (Protected CHX-A″-octreotide).** Prepared by the general solution-phase method; a retention time of 30 min on RP-HPLC under acidic solvent gradient system (aqeuous 1% TFA with increasing CH_3CN gradient) (Figure 4); ES-MS of $C_{104}H_{154}N_{14}O_{24}S_2$: [M + 2H$^+$] requires, 1024.54; found, 1025.10.

***N*-[CHX-A″]-(Cys2-Cys7)-D-Phe-Cys-Phe-D-Trp-Lys-Thr-Cys-Thr-ol (CHX-A″-octreotide).** After TFA deprotection; retention time of 24 min on RP-HPLC under neutral solvent gradient system (aqueous NH_4OAc with increasing CH_3CN gradient) (Figure 5); ES-MS of $C_{79}H_{106}N_{14}O_{22}S_2$: [M + Na$^+$ + K$^+$] requires, 864.33; found, 864.54.

Acknowledgment. This research was supported in part by the Intramural Research Program of the NIH, National Cancer Institute, and the Center for Cancer Research. The production of ^{86}Y at Washington University was supported by a grant from the National Cancer Institute (R24 CA86307; M.J. Welch, P.I.).

Supporting Information Available: ^{1}H, ^{13}C, and 2D-COSY NMR spectra, ESI mass spectra, elemental analysis results of relevant intermediates and compounds, and biodistribution data (4 and 24 h) for ^{86}Y-CHX-A″-octreotide in AR42J tumor-bearing rats in tabular format. This information is available free of charge via the Internet at http://pubs.acs.org.

References

(1) Milenic, D. E.; Brady, E. D.; Brechbiel, M. W. Antibody-targeted radiation cancer therapy. *Nat. Rev. Drug Discovery* **2004**, *3*, 488−499.

(2) Blend, M. J.; Stastny, J. J.; Swanson, S. M.; Brechbiel, M. W. Labeling anti-HER2/neu monoclonal antibodies with ^{111}In and ^{90}Y using a bifunctional DTPA chelating agent. *Cancer Biother. Radiopharm.* **2003**, *18*, 355−363.

(3) Parry, R.; Schneider, D.; Hudson, D.; Parkes, D.; Xuan, J.; Newton, A.; Toy, P.; Lin, R.; Harkins, R.; Alicke, B.; Biroc, S.; Kretschmer, P. J.; Halks-Miller, M.; Klocker, H.; Zhu, Y.; Larsen, B.; Cobb, R. R.; Bringmann, P.; Roth, G.; Lewis, J. S.; Dinter, H.; Parry, G. Identification of a novel prostate tumor target, Mindin/RG-1, for antibody-based radiotherapy of prostate cancer. *Cancer Res.* **2005**, *65*, 8397−8405.

(4) Lee, F. T.; Mountain, A. J.; Kelly, M. P.; Hall, C.; Rigopoulos, A.; Johns, T. G.; Smyth, F. E.; Brechbiel, M. W.; Nice, E. C.; Burgess, A. W.; Scott, A. M. Enhanced efficacy of radioimmunotherapy with ^{90}Y-CHX-A″-DTPA-hu3S193 by inhibition of epidermal growth factor receptor (EGFR) signaling with EGFR tyrosine kinase inhibitor AG1478. *Clin. Cancer Res.* **2005**, *11*, 7080−7086.

(5) Chong, H. S.; Garmestani, K.; Ma, D. S.; Milenic, D. E.; Overstreet, T.; Brechbiel, M. W. Synthesis and biological evaluation of novel macrocyclic ligands with pendant donor groups as potential yttrium chelators for radioimmunotherapy with improved complex formation kinetics. *J. Med. Chem.* **2002**, *45*, 3458−3464.

(6) Wu, C.; Virzi, F.; Hnatowich, D. J. Investigations of *N*-linked macrocycles for ^{111}In and ^{90}Y labeling of proteins. *Nucl. Med. Biol.* **1992**, *19*, 239−244.

(7) Ruegg, C. L.; Anderson-Berg, W. T.; Brechbiel, M. W.; Mirzadeh, S.; Gansow, O. A.; Strand, M. Improved in vivo stability and tumor targeting of bismuth-labeled antibody. *Cancer Res.* **1990**, *50*, 4221−4226.

(8) Milenic, D. E.; Roselli, M.; Mirzadeh, S.; Pippen, C. G.; Gansow, O. A.; Colcher, D.; Brechbiel, M. W.; Schlom, J. In vivo evaluation of bismuth-labeled monoclonal antibody comparing DTPA-derived bifunctional chelates. *Cancer Biother. Radiopharm.* **2001**, *16*, 133−146.

(9) Brechbiel, M. W.; Gansow, O. A.; Pippen, C. G.; Rogers, R. D.; Planalp, R. P. Preparation of the novel chelating agent *N*-(2-aminoethyl)-*trans*-1,2-diaminocyclohexane-*N*,*N*′,*N*″-pentaacetic acid (H_5CyDTPA), a preorganized analogue of diethylenetriaminepentaacetic acid (H_5DTPA), and the structures of Bi^{III}(CyDTPA)$^{2-}$ and $Bi^{III}(H_2$DTPA) complexes. *Inorg. Chem.* **1996**, *35*, 6343−6348.

(10) Wu, C.; Kobayashi, H.; Sun, B.; Yoo, T. M.; Paik, C. H.; Gansow, O. A.; Carrasquillo, J. A.; Pastan, I.; Brechbiel, M. W. Stereochemical influence on the stability of radio-metal complexes in vivo. Synthesis and evaluation of the four stereoisomers of 2-(*p*-nitrobenzyl)-trans-CyDTPA. *Bioorg. Med. Chem. Lett.* **1997**, *5*, 1925−1934.

(11) Kobayashi, H.; Wu, C. C.; Yoo, T. M.; Sun, B. F.; Drumm, D.; Pastan, I.; Paik, C. H.; Gansow, O. A.; Carrasquillo, J. A.; Brechbiel, M. W. Evaluation of the in vivo biodistribution of yttrium-labeled isomers of CHX-DTPA-conjugated monoclonal antibodies. *J. Nucl. Med.* **1998**, *39*, 829−836.

(12) Milenic, D. E.; Garmestani, K.; Brady, E. D.; Albert, P. S.; Ma, D. S.; Abdulla, A.; Brechbiel, M. W. Targeting of HER2 antigen for the treatment of disseminated peritoneal disease. *Clin. Cancer Res.* **2004**, *10*, 7834−7841.

(13) Milenic, D. E.; Garmestani, K.; Brady, E. D.; Albert, P. S.; Ma, D.; Abdulla, A.; Brechbiel, M. W. α-Particle radioimmunotherapy of disseminated peritoneal disease using a ^{212}Pb-labeled radioimmunoconjugate targeting HER2. *Cancer Biother. Radiopharm.* **2005**, *20*, 557−568.

(14) Li, W. P.; Meyer, L. A.; Anderson, C. J. Contrast agents III: Radiopharmaceuticals − From diagnostics to therapeutics. *Top. Curr. Chem.* **2005**, *252*, 179−192.

(15) Reubi, J. C. Peptide receptors as molecular targets for cancer diagnosis and therapy. *Endocrine Rev.* **2003**, *24*, 389−427.

(16) Blok, D.; Feitsma, R. I. J.; Vermeij, P.; Pauwels, E. J. K. Peptide radiopharmaceuticals in nuclear medicine. *Eur. J. Nucl. Med.* **1999**, *26*, 1511−1519.

(17) Heppeler, A.; Froidevaux, S.; Eberle, A. N.; Maecke, H. R. Receptor targeting for tumor localisation and therapy with radiopeptides. *Curr. Med. Chem.* **2000**, *7*, 971−994.

(18) Reichlin, S. Somatostatin (part 1). *N. Engl. J. Med.* **1983**, *309*, 1495−1501.

(19) Reichlin, S. Somatostatin (part 2). *N. Engl. J. Med.* **1983**, *309*, 1556−1563.

(20) Reubi, J. C.; Kvols, L. K.; Krenning, E. P.; Lamberts, S. W. J. Distribution of somatostatin receptors in normal and tumor tissue. *Metabolism (supplement 2)* **1990**, *39*, 78−81.

(21) Dasgupta, P. Somatostatin analogs: Multiple roles in cellular proliferation, neoplasia, and angiogenesis. *Pharmacol.Ther.* **2004**, *102*, 61−85.

(22) Deshmukh, M. V.; Voll, G.; Kuhlewein, A.; Maecke, H.; Schmitt, J.; Kessler, H.; Gemmecker, G. NMR studies reveal structural differences between the gallium and yttrium complexes of DOTA-D-Phe^1-Tyr^3-octreotide. *J. Med. Chem.* **2005**, *48*, 1506−1514.

(23) Wang, W.; McMurray, J. S.; Wu, Q.; Campbell, M. L.; Li, C. Convenient solid-phase synthesis of diethylenetriaminepenta-acetic acid (DTPA)-conjugated cyclic RGD peptide analogs. *Cancer Biother. Radiopharm.* **2005**, *20*, 547−556.

(24) Brechbiel, M. W.; Gansow, O. A.; Atcher, R. W.; Schlom, J.; Esteban, J.; Simpson, D. E.; Colcher, D. Synthesis of 1-(*p*-Isothiocyanatobenzyl) derivatives of DTPA and EDTA. Antibody labeling and tumor-imaging studies. *Inorg. Chem.* **1986**, *25*, 2772−2781.

(25) Mirzadeh, S.; Brechbiel, M. W.; Atcher, R. W.; Gansow, O. A. Radiometal labeling of immunoproteins: Covalent linkage of 2-(4-isothiocyanatobenzyl)diethylenetriaminepentaacetic acid ligands to immunoglobulin. *Bioconjugate Chem.* **1990**, *1*, 59−65.

(26) Song, A. I.; Rana, T. M. Synthesis of an amino acid analog to incorporate *p*-aminobenzyl-EDTA in peptides. *Bioconjugate Chem.* **1997**, *8*, 249−252.

(27) Riddoch, R. W.; Schaffer, P.; Valliant, J. F. A solid-phase labeling strategy for the preparation of technetium and rhenium bifunctional chelate complexes and associated peptide conjugates. *Bioconjugate Chem.* **2006**, *17*, 226−235.

(28) Stephenson, K. A.; Zubieta, J.; Banerjee, S. R.; Levadala, M. K.; Taggart, L.; Ryan, L.; McFarlane, N.; Boreham, D. R.; Maresca, K. P.; Babich, J. W.; Valliant, J. F. A new strategy for the preparation of peptide-targeted radiopharmaceuticals based on an Fmoc-lysine-derived single amino acid chelate (SAAC). Automated solid-phase synthesis, NMR characterization, and in vitro screening of fMLF-(SAAC)G and fMLF[(SAAC-Re(CO)$_3$)$^+$]G. *Bioconjugate Chem.* **2004**, *15*, 128−136.

(29) Stimmel, J. B.; Stockstill, M. E.; Kull, F. C. Y-90 chelation properties of tetraazatetraacetic acid macrocycles, diethylenetriaminepentaacetic acid analogs, and a novel terpyridine acyclic chelator. *Bioconjugate Chem.* **1995**, *6*, 219−225.

(30) Boswell, C. A.; Brechbiel, M. W. Auger electrons: lethal, low energy, and coming soon to a tumor cell nucleus near you. *J. Nucl. Med.* **2005**, *46*, 1946−1947.
(31) Krenning, E. P.; Kooij, P. P. M.; Bakker, W. H.; Breeman, W. A. P.; Postema, P. T. E.; Kwekkeboom, D. J.; Oei, H. Y.; de Jong, M.; Visser, T. J.; Reijs, A. E. M.; Lamberts, S. W. J. Radiotherapy with a radiolabeled somatostatin analog, ^{111}In-DTPA-Phe^{1}-octreotide: A case history. *Ann. N.Y. Acad. Sci.* **1994**, *733*, 496−506.
(32) Fjälling, M.; Andersson, P.; Forsell-Aronsson, E.; Grétarsdóttir, J.; Johansson, V.; Tisell, L. E.; Wängber, B.; Nilsson, O.; Berg, A.; Michanek, A.; Glindstedt, G.; Ahlman, H. Systemic radionuclide therapy using ^{111}In-DTPA-D-Phe^{1}-octreotide in midgut carcinoid syndrome. *J. Nucl. Med.* **1996**, *37*, 1519−1521.
(33) Bakker, W. H.; Albert, R.; Bruns, C.; Breeman, W. A. P.; Hofland, L. J.; Marbach, P.; Pless, J.; Pralet, D.; Stolz, B.; Koper, J. W.; Lamberts, S. W. J.; Visser, T. J.; Krenning, E. P. [^{111}In-DTPA-D-Phe]-octreotide, a potential radiopharmaceutical for imaging of somatostatin receptor-positive tumors: synthesis, radiolabeling and in vitro validation. *Life Sci.* **1991**, *49*, 1583−1591.
(34) Bakker, W. H.; Krenning, E. P.; Reubi, J. C.; Breeman, W. A. P.; Setyono-Han, B.; de Jong, M.; Kooij, P. P. M.; Bruns, C.; van Hagen, P. M.; Marbach, P.; Visser, T. J.; Pless, J.; Lamberts, S. W. J. In vivo application of [^{111}In-DTPA-D-Phe]-octreotide for detection of somatostatin receptor-positive tumors in rats. *Life Sci.* **1991**, *49*, 1593−1601.
(35) Krenning, E. P.; Bakker, W. H.; Kooij, P. P. M.; Breeman, W. A. P.; Oei, H. Y.; de Jong, M.; Reubi, J. C.; Visser, T. J.; Bruns, C.; Kwekkeboom, D. J.; Reijs, A. E. M.; van Hagen, P. M.; Koper, J. W.; Lamberts, S. W. J. Somatostatin receptor scintigraphy with ^{111}In-DTPA-D-Phe^{1}-octreotide in man: Metabolism, dosimetry and comparison with ^{123}I-Tyr^{3}-octreotide. *J. Nucl. Med.* **1992**, *33*, 652−658.
(36) Rolleman, E. J.; Valkema, R.; de Jong, M.; Kooij, P. P. M.; Krenning, E. P. Safe and effective inhibition of renal uptake of radiolabeled octreotide by a combination of lysine and arginine. *Eur. J. Nucl. Med. Mol. Imaging* **2003**, *30*, 9−15.
(37) Stolz, B.; Smith-Jones, P.; Albert, R.; Tolcsvai, L.; Briner, U.; Ruser, G.; Mäcke, H.; Weckbecker, G.; Bruns, C. Somatostatin analogs for somatostatin-receptor-mediated radiotherapy of cancer. *Digestion* **1996**, *57*, 17−21.
(38) Stolz, B.; Weckbecker, G.; Smith-Jones, P. M.; Albert, R.; Raulf, F.; Bruns, C. The somatostatin receptor-targeted radiotherapeutic [^{90}Y-DOTA-DPhe^{1},Tyr^{3}]octreotide (^{90}Y-SMT 487) eradicates experimental rat pancreatic CA 20948 tumours. *Eur. J. Nucl. Med.* **1998**, *25*, 668−674.
(39) Otte, A.; Muellerbrand, J.; Dellas, S.; Nitzsche, E. U.; Herrmann, R.; Maecke, H. R. Yttrium-90-labeled somatostatin analog for cancer treatment. *Lancet* **1998**, *351*, 417−418.
(40) Jamar, F.; Barone, R.; Mathieu, I.; Walrand, S.; Labar, D.; Carlier, P.; de Camps, J.; Schran, H.; Chen, T.; Smith, M. C.; Bouterfa, H.; Valkema, R.; Krenning, E. P.; Kvols, L. K.; Pauwels, S. Y-86-DOTA^{0}-D-Phe^{1}-Tyr^{3}-octreotide (SMT487) − A Phase 1 clinical study: Pharmacokinetics, biodistribution and renal protective effect of different regimens of amino acid co-infusion. *Eur. J. Nucl. Med.* **2003**, *30*, 510−518.
(41) Mansi, L. From the magic bullet experience to an effective therapy: The peptide experience. *Eur. J. Nucl. Med. Mol. Imaging* **2004**, *31*, 1393−1398.
(42) Goddu, S. M.; Rao, D. V.; Howell, R. W. Multicellular dosimetry for micrometastases: dependence of self-dose versus cross-dose to cell nuclei on type and energy of radiation and subcellular distribution of radionuclides. *J. Nucl. Med.* **1994**, *35*, 521−530.
(43) Carrasquillo, J. A.; White, J. D.; Paik, C. H.; Raubitschek, A.; Le, N.; Rotman, M.; Brechbiel, M. W.; Gansow, O.; Top, L. E.; Perentesis, P.; Reynolds, J. C.; Nelson, D. L.; Waldmann, T. A. Similarities and differences in ^{111}In- and ^{90}Y-labeled 1B4M-DTPA antiTac monoclonal antibody distribution. *J. Nucl. Med.* **1999**, *40*, 268−276.
(44) Pai-Scherf, L. H.; Carrasquillo, J. A.; Paik, C. H.; Gansow, O.; Whatley, M.; Pearson, D. A.; Webber, K.; Hamilton, M.; Allegra, C.; Brechbiel, M. W.; Willingham, M. C.; Pastan, I. Imaging and phase I study of ^{111}In- and ^{90}Y-labeled anti-LewisY monoclonal antibody B3. *Clin. Cancer Res.* **2000**, *6*, 1720−1730.
(45) Herzog, H.; Rosch, F.; Stocklin, G.; Lueders, C.; Qaim, S. M.; Feinendegen, L. E. Measurement of pharmacokinetics of ^{86}Y radiopharmaceuticals with PET and radiation dose calculation of analogous ^{90}Y radiotherapeutics. *J. Nucl. Med.* **1993**, *34*, 2222−2226.
(46) Rösch, F.; Qaim, S. M.; Stöcklin, G. Production of the positron emitting radioisotope ^{86}Y for nuclear medicine application. *Appl. Radiat. Isot.* **1993**, *44*, 677−681.
(47) Garmestani, K.; Milenic, D. E.; Plascjak, P. S.; Brechbiel, M. W. A new and convenient method for purification of ^{86}Y using a Sr(II) selective resin and comparison of biodistribution of ^{86}Y and ^{111}In labeled Herceptin. *Nucl. Med. Biol.* **2002**, *29*, 599−606.
(48) Park, L. S.; Szajek, L. P.; Wong, K. J.; Pascjak, P. S.; Garmestani, K.; Googins, S.; Eckelman, W. C.; Carrasquillo, J. A.; Paik, C. H. Semi-automated ^{86}Y purification using a three-column system. *Nucl. Med. Biol.* **2004**, *31*, 297−301.
(49) Reischl, G.; Rosch, F.; Machulla, H. Electrochemical separation and purification of ^{86}Y. *Radiochim. Acta* **2002**, *90*, 225−228.
(50) Yoo, J.; Tang, L.; Perkins, T. A.; Rowland, D. J.; Laforest, R.; Lewis, J. S.; Welch, M. J. Preparation of high specific activity ^{86}Y using a small biomedical cyclotron. *Nucl. Med. Biol.* **2005**, *32*, 891−897.
(51) McQuade, P.; Miao, Y.; Yoo, J.; Quinn, T. P.; Welch, M. J.; Lewis, J. S. Imaging of melanoma using ^{64}Cu- and ^{86}Y-DOTA-ReCCMSH-(Arg^{11}), a cyclized peptide analogue of α-MSH. *J. Med. Chem.* **2005**, *48*, 2985−2992.
(52) Boswell, C. A.; Sun, X.; Niu, W.; Weisman, G. R.; Wong, E. H.; Rheingold, A. L.; Anderson, C. J. Comparative in vivo stability of ^{64}Cu-labeled cross-bridged and conventional tetraazamacrocyclic complexes. *J. Med. Chem.* **2004**, *47*, 1465−1474.
(53) Lewis, J. S.; Lewis, M. R.; Cutler, P. D.; Srinivasan, A.; Schmidt, M. A.; Schwarz, S. W.; Morris, M. M.; Miller, J. P.; Anderson, C. J. Radiotherapy and dosimetry of ^{64}Cu-TETA-Tyr3-octreotate in a somatostatin receptor-positive tumor-bearing rat model. *Clin. Cancer Res.* **1999**, *5*, 3608−3616.
(54) Breeman, W. A. P.; Kwekkeboom, D. J.; Kooij, P. P. M.; Bakker, W. H.; Hofland, L. J.; Visser, T. J.; Ensing, G. J.; Lamberts, S. W. J.; Krenning, E. P. Effect of dose and specific acitivity on tissue distribution of ^{111}In-pentetreotide in rats. *J. Nucl. Med.* **1995**, *36*, 623−627.
(55) Norenberg, J. P.; Krenning, B. J.; Konings, I. R. H. M.; Kusewitt, D. F.; Nayak, T. K.; Anderson, T. L.; de Jong, M.; Garmestani, K.; Brechbiel, M. W.; Kvols, L. K. Bi-213-[DOTA(0),Tyr(3)]octreotide peptide receptor radionuclide therapy of pancreatic tumors in a preclinical animal model. *Clin. Cancer Res.* **2006**, *12*, 897−903.

JM060317V